Chemical Science

Cite this: *Chem. Sci.*, 2012, **3**, 1313

www.rsc.org/chemicalscience

EDGE ARTICLE

Thermally stable N_2 and H_2 adducts of cationic nickel(II)†

Charlene Tsay and Jonas C. Peters*

Received 8th December 2011, Accepted 18th January 2012
DOI: 10.1039/c2sc01033j

The first examples of thermally stable molecular dihydrogen adducts of nickel were synthesized from their dinitrogen adduct precursors, which are themselves among the first examples of Ni(II)-N_2 complexes. The minimal activation of the bound N_2 moieties suggests that these adducts are stabilized predominantly through σ-donation from the adduct to the electrophilic metal center. We further show that the bound H_2 ligand can undergo heterolytic cleavage to deliver hydride to the nickel center. The H_2 adducts are of particular interest in the context of hypotheses suggesting that Ni can serve as the site for H_2 binding and heterolytic activation in [NiFe] hydrogenases.

Introduction

Dihydrogen complexes of late first-row transition metals such as Co, Ni, and Cu are extremely uncommon and typically subject to facile heterolysis.[1] Nickel dihydrogen adducts have been studied theoretically[2] and detected in bulk metal and microporous materials as well as under gas phase and matrix isolation conditions,[3] but have not been isolated as stable species. The only reported molecular example is a $[PNP]Ni(H_2)^+$ intermediate detected at low temperatures by Caulton and co-workers; the H_2 subsequently undergoes intramolecular heterolytic cleavage.[4]

Due to the lack of stable $Ni(H_2)$ complexes and the relative scarcity of nickel hydrides,[1] iron is often proposed to be the site of dihydrogen binding and heterolytic activation in [NiFe] hydrogenases.[5,6] However, certain EPR, X-ray diffraction and theoretical studies have been interpreted to suggest that H_2 is instead activated at a five-coordinate, EPR-silent Ni center in the enzyme active site.[7] Moreover, relatively efficient hydrogenase activity, both for H_2 oxidation and proton reduction, has been demonstrated for model compounds of nickel,[8] particularly the macrocyclic $Ni(P_2N_2)_2$ systems pioneered by DuBois and co-workers.[8b] The presumed initial H_2-adducts have not yet been isolated or detected in these catalytically competent systems.

Herein we report examples of thermally stable dihydrogen adducts of nickel and show that the bound H_2 ligand can undergo intermolecular heterolytic cleavage to deliver hydride to the nickel center when the auxiliary ligand is appropriately chosen. Access to these Ni(II)-(H_2) complexes proceeds from their Ni(II)-(N_2) adduct precursors, which are themselves highly unusual species. Dinitrogen complexes of nickel are rare in general.[9,10] With the exception of a recently reported $Ni(N_2)$ compound featuring a redox-active diiminopyridine ligand,[11] examples of N_2 complexes of Ni(II) have, to our knowledge, only been observed in low-temperature matrices.[12]

Division of Chemistry and Chemical Engineering, California Institute of Technology, Pasadena, CA, 91125, USA. E-mail: jpeters@caltech.edu

† Electronic supplementary information (ESI) available: Synthetic, spectroscopic, and crystallographic details. CCDC reference numbers 844852–844858. For ESI and crystallographic data in CIF or other electronic format see DOI: 10.1039/c2sc01033j

Results and discussion

Access to cationic dinitrogen adducts of Ni(II)

The mono-anionic, tetradentate tris(phosphino)silyl ligand $[SiP^R_3]$ ($[SiP^R_3] = [(2\text{-}R_2PC_6H_4)_3Si]^-$; R = Ph, ^{i}Pr)[13] affords access to the chemistry of interest herein. We previously established the efficacy of this ligand in supporting highly electrophilic, trigonal-pyramidal cations of Pt(II) and Pd(II), as well as cationic Pt-(H_2) adducts.[14] We conjectured that this ligand scaffold might also enable access to stable dihydrogen adducts of nickel. Accordingly, $[SiP^{iPr}_3]Ni\text{–}CH_3$ (**1a**) was synthesized by the addition of MeLi to the previously reported $[SiP^{iPr}_3]Ni\text{–}Cl$.[15] The analogous methyl compound of the less electron-rich, phenyl-substituted ligand, $[SiP^{Ph}_3]Ni\text{–}CH_3$ (**1b**), was synthesized by the addition of excess MeMgCl to $NiCl_2\cdot DME$ and the free ligand $H[SiP^{Ph}_3]$.[13] These compounds retain their three-fold symmetry in solution, as evidenced by single, sharp $^{31}P\{^1H\}$ resonances at 43.9 and 45.9 ppm, respectively.

Upon protonation of **1a** with $H(OEt_2)_2BAr^F_4$ (BAr^F_4 = B[3,5-$(CF_3)_2C_6H_3]_4$) in CH_2Cl_2 under an N_2 atmosphere, the room-temperature (RT) $^{31}P\{^1H\}$ NMR spectrum of the dark brown solution shows a very broad peak centered around 46.2 ppm that sharpens upon cooling below −10 °C. When the protonation is performed in C_6H_6, the product can be isolated as an orange precipitate that reversibly turns dark pink under vacuum, suggesting the coordination of dinitrogen to the nickel cation.

The solid-state structure of a single crystal of this material, obtained from slow evaporation of a CH_2Cl_2 solution, confirms N_2 coordination in the trigonal-bipyramidal cation $\{[SiP^{iPr}_3]Ni(N_2)\}\{BAr^F_4\}$ (**2a**) (Scheme 1, Fig. 1). The apical dinitrogen moiety is bound end-on with a short N–N distance of 1.087(2) Å. An extremely high N–N stretching frequency is observed in the

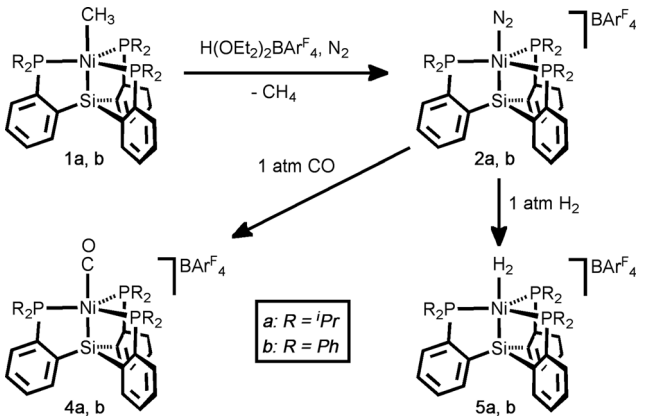

Scheme 1

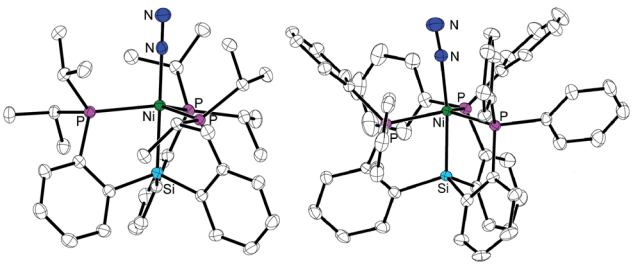

Fig. 1 Solid-state structures of cations **2a** (left) and **2b** (right). Thermal ellipsoids drawn at 50% probability. Hydrogen atoms and BAr^F_4 anions omitted for clarity. Selected distances (Å) and angles (°) for **2a**: Ni–N 1.905(2), N–N 1.087(2); Si–Ni–N 178.63(5), Ni–N–N 179.8(2); **2b**: Ni–N 1.891(2), N–N 1.083(3); Si–Ni–N 172.87(7), Ni–N–N 175.2(2).

solid-state IR spectrum at 2223 cm^{-1} and attests to minimal activation of the N–N bond through back-bonding from the cationic Ni center. While the cationic charge of the metal center attenuates the degree of back-bonding to the N_2 moiety, its electrophilicity likely facilitates σ-donation from the N_2 to the empty d_{z^2} orbital, strengthening the M–N_2 interaction; the relative stability of this species in the solid-state raises the possibility that σ-donation can contribute more significantly to the M–N_2 interaction than π back-bonding.[16] The fact that the N–N distance observed in the solid state is shorter than that of free N_2 may also indicate that the interaction is predominantly N_2 σ-donation to the metal, with minimal π back-bonding.[17,18] $^{15}N\{^1H\}$ NMR spectroscopy of the labeled analogue **2a′** at −40 °C reveals resonances at 361.8 and 310.4 ppm (Fig. 2). Dichloromethane solutions of **2a** decompose gradually over days to paramagnetic {[SiP^{iPr}_3]Ni(III)–Cl}{BAr^F_4}, a species whose identity was determined by a low-resolution X-ray diffraction study. Complex **2a** can nevertheless be obtained in analytically pure form and stored in pentane at −30 °C under nitrogen.

Protonation of **1b** with $H(OEt_2)_2BAr^F_4$ in benzene generates the analogous dinitrogen adduct, {[SiP^{Ph}_3]Ni(N_2)}{BAr^F_4} (**2b**) (Scheme 1, Fig. 1), which exhibits an even more weakly activated N_2 ligand with an N–N stretching frequency of 2234 cm^{-1} in the solid state. A sharp singlet is observed at 42.5 ppm in the $^{31}P\{^1H\}$ NMR spectrum at RT, indicating that the N_2 moiety in **2b** is bound more strongly than that in **2a**. Labeling with $^{15}N_2$ results in $^{15}N\{^1H\}$ NMR shifts of 346.9 and 296.9 ppm at −20 °C

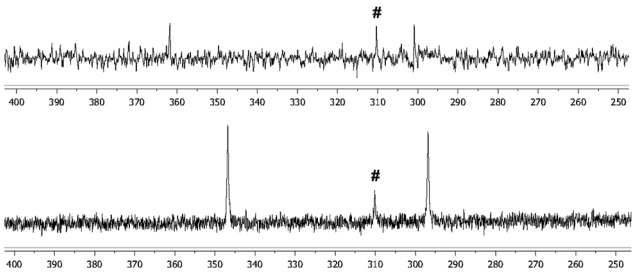

Fig. 2 ^{15}N NMR spectra of N_2 adducts **2a′** in CD_2Cl_2 at −40 °C (top) and **2b′** in toluene-d_8 at −20 °C (bottom). Chemical shifts in ppm, referenced to liquid NH_3 at 0 ppm. Peaks marked with a '#' symbol are from free dinitrogen in solution.

(Fig. 2). Single crystals of **2b** were obtained by diffusion of pentane vapors into a benzene solution, and an X-ray diffraction study revealed an N–N distance of 1.083(3) Å. Again, the extremely short N–N bond and its high stretching frequency show the effect of both the σ-donation from the N_2 and the minimal π back-bonding from the Ni center. Solid samples of **2b** can be isolated by performing the protonation in pentane spiked with minimal benzene; the resulting orange solid does not change color under vacuum, in contrast to **2a**. This increased stability is counterintuitive, given the weaker activation of the N_2 ligand; it is, however, consistent with a stronger M–N_2 interaction arising from stronger σ-donation from N_2 to a more electrophilic metal center.

Of the few isolable Ni(N_2) compounds reported in the literature, the three that to our knowledge feature terminal dinitrogen ligands bound end-on to the metal are shown in Scheme 2. The first reported Ni(N_2) compound,[10a] crystallographically characterized as the dimeric [$(Cy_3P)_2$Ni–(N_2)–Ni(PCy_3)$_2$], dissociates in solution to give a terminal dinitrogen bound end-on to a Ni(0) center, with an N–N stretching frequency of 2028 cm^{-1}. The Ni(0) (dtbpe)Ni(N_2)(PPh_3) complex[10b] exhibits a similar N–N stretch of 2072 cm^{-1}. A terminal, end-on Ni–N_2 species with a redox-active diiminopyridine ligand was recently reported;[11] the observed N–N stretch of 2156 cm^{-1} corroborates the interpretation of its electronic structure as a Ni(II) center coupled to a dianionic ligand. The extremely high N–N stretches for the cationic Ni(II) compounds **2a** and **2b** are in line with N–N stretches of η^1-N_2 adducts of NiX_2 observed in low-temperature nitrogen matrices (Table 1).[12d]

The solid-state Ni–N distances of the end-on N_2 adducts (Table 2), which may be reflective of the Ni–N bond strength, also reflect the contributions of both σ-donation and π back-bonding. The Ni(0) (dtbpe)Ni(N_2)(PPh_3) complex exhibits a Ni–N distance of 1.830(2) Å, while the more electrophilic

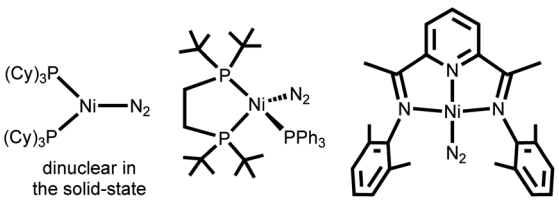

Scheme 2

Table 1 Dinitrogen stretching frequencies for end-on Ni(N_2) complexes

Complex	ν_{N-N}/cm^{-1}	Ref.
$[(Cy_3P)_2Ni–(N_2)–Ni(PCy_3)_2]^a$	2028	10*a*
$(dtbpe)Ni(N_2)(PPh_3)^b$	2072	10*b*
$[DIMPY]Ni(N_2)^c$	2156	11
$[SiP^{iPr}_3]Ni(N_2)^+$ (**2a**)	2223	This work
$[SiP^{Ph}_3]Ni(N_2)^+$ (**2b**)	2234	This work
$NiCl_2(N_2)_2^d$	2281, 2260	12*d*
$NiBr_2(N_2)_2^d$	2281, 2261	12*d*

[a] Monomeric in solution. [b] dtbpe = 1,2-bis(di-*tert*-butylphosphino)-ethane). [c] DIMPY = 2,6-bis[1-(2,6-diisopropylphenylimino)ethyl] pyridine. [d] Observed in solid N_2 matrices below 10 K.

Table 2 Solid-state metal–N distances in selected end-on M–N_2 complexes

Complex	M–N distance/Å	Ref.
$(dtbpe)Ni(N_2)(PPh_3)$	1.830(2)[a]	10*b*
$[DIMPY]Ni(N_2)$	1.908(9)[b]	11
$[SiP^{iPr}_3]Ni(N_2)^+$ (**2a**)	1.905(2)[a]	This work
$[SiP^{Ph}_3]Ni(N_2)^+$ (**2b**)	1.891(2)[a]	This work
$[SiP^{iPr}_3]Co(N_2)$	1.813(2)[a]	15

[a] Data collected at 100 K. [b] Data collected at 200 K.

Ni(II) complexes, $[DIMPY]Ni(N_2)$, **2a** and **2b**, have an average Ni–N distance of 1.90 Å; this trend is consistent with stronger, shorter M–N bonds arising from increased back-bonding in the more electron-rich compounds. This is additionally illustrated by the short Co–N distance of 1.813(2) Å in the previously reported $[SiP^{iPr}_3]Co(N_2)$.[15] While this Co(I) compound is isoelectronic with **2a** and **2b**, its neutral charge allows for stronger back-bonding and a correspondingly shorter M–N bond. The more subtle effect of σ-donation can perhaps be seen in the Ni–N bond distances of **2a** and **2b**. Though the Ni center in **2a** is more electron-rich, its Ni–N distance is longer than that in **2b**. Increased σ-donation thus seems to be able to compensate for decreased π back-bonding in stabilizing the M–N_2 bonding interaction, at least under the assumption that the M–N bond distances of N_2 complexes reflect the M–N_2 bonding interaction.

Addition of acetonitrile to the N_2-adduct **2a** generates the solvento species $\{[SiP^{iPr}_3]Ni(NCMe)\}\{BAr^F_4\}$ (**3a**), and exposure to an atmosphere of CO affords the CO-adduct $\{[SiP^{iPr}_3]Ni(CO)\}\{BAr^F_4\}$ (**4a**) (Scheme 1).[19] A C–O distance of 1.157(8) Å was obtained from a single crystal grown by slow evaporation of a CH_2Cl_2 solution of **4a** (Fig. 3). Similarly, an atmosphere of CO displaces the N_2 ligand of **2b** in solution and generates the cationic adduct $\{[SiP^{Ph}_3]Ni(CO)\}\{BAr^F_4\}$ (**4b**); the crystal structure, obtained from layering pentane on a benzene solution, reveals a C–O distance of 1.137(3) Å (Scheme 1, Fig. 3). The high C–O stretching frequencies of 2036 and 2046 cm^{-1} in the solid-state IR spectra of **4a** and **4b**, respectively, are further evidence of the very weak back-bonding ability of the cationic nickel centers, and can be compared to the 2056 cm^{-1} stretch observed in [NiFe] hydrogenase for the Ni–bound, exogenous CO moiety that inhibits activity.[20]

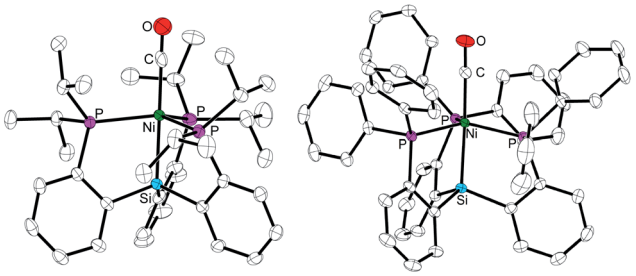

Fig. 3 Solid-state structures of cations **4a** (left) and **4b** (right). Thermal ellipsoids drawn at 50% probability. Hydrogen atoms and BAr^F_4 anions omitted for clarity. Selected distances (Å) and angles (°) for **4a**: Ni–C 1.787(4), C–O 1.157(8); Si–Ni–C 178.9(2), Ni–C–O 178.7(4); **4b**: Ni–C 1.796(2), C–O 1.137(3); Si–Ni–C 172.56(7), Ni–C–O 175.9(2).

Thermally stable, cationic dihydrogen adducts of Ni(II)

The labile N_2 ligand of **2a** is readily displaced in solution upon exposure to one atmosphere of H_2 to form $\{[SiP^{iPr}_3]Ni(H_2)\}\{BAr^F_4\}$ (**5a**) (Scheme 1). The yellow cationic product features a resonance in its ^{1}H NMR spectrum at RT that is centered at −3.58 ppm and integrates to two H-atoms. NMR spectroscopic parameters that include a T_1(min) of 20 ms (−50 °C, 500 MHz) for **5a** and a $^1J_{H\text{-}D}$ of 35 Hz for its HD analogue **5a′** (Fig. 4) are diagnostic of an intact H_2 ligand.[21,1] The more tightly-bound N_2 ligand of **2b** is also rapidly displaced by an atmosphere of H_2 to generate $\{[SiP^{Ph}_3]Ni(H_2)\}\{BAr^F_4\}$ (**5b**). The bound dihydrogen in **5b** exhibits a T_1(min) of 24 ms (30 °C, 500 MHz) and $^1J_{H\text{-}D}$ of 33 Hz for the HD analogue **5b′** (Fig. 4); these values again indicate an intact H_2 ligand.

The ^{1}H NMR resonances corresponding to free H_2 in solution in the VT spectra of **5a** and **5b** offer an indirect gauge of the strength of the Ni–H_2 interaction. No free H_2 peak is observed in

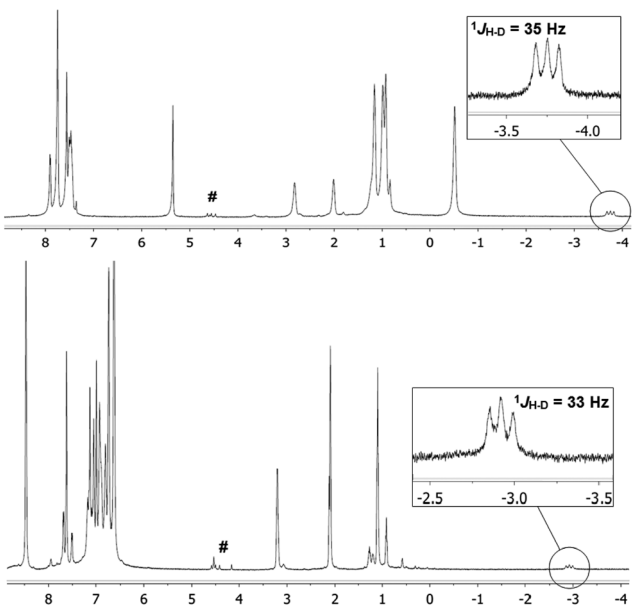

Fig. 4 ^{1}H NMR spectrum of HD adducts **5a′** in CD_2Cl_2 at −70 °C (top) and **5b′** in toluene-d_8 at −20 °C (bottom). Chemical shifts in ppm. Peaks marked with a '#' symbol are from free H_2 (singlet) and HD (three-line pattern) in solution.

the RT ^{1}H spectrum of **5b** and the bound dihydrogen peak is extremely broad, indicating rapid exchange between bound and free H_2. The free H_2 resonance appears upon cooling to −10 °C and sharpens at −20 °C (Fig. S5d, ESI†). In contrast, free H_2 is observed in the RT spectrum of **5a**, though both it and the bound dihydrogen peak are broad; both peaks sharpen up at 10 °C (Fig. S4d, ESI†). This suggests that the dihydrogen ligand is bound more strongly in **5a**, most likely due to stronger back-bonding from the comparatively more electron-rich metal center. This trend of stability is in contrast to the relative stabilities of the N_2 complexes, and suggests that π back-bonding, though minimal in these complexes, may have a more significant effect on the strength of the Ni–H_2 interaction than that of the Ni–N_2 interaction.

While we have not yet been able to obtain solid-state structures of **5a** and **5b**, the DFT optimized structures (Fig. 5) provide a basis for some qualitative comparisons. Both structures feature short H–H bonds consistent with the short T_1(min) and large $^1J_{H\text{-}D}$ values obtained experimentally. The Ni–H distances in the relatively electron-rich **5a** are slightly shorter than those in **5b**, which is also consistent with the experimental observations described above.

Intramolecular heterolytic activation of the coordinated H_2 ligand in **5a** would presumably deliver hydride to the nickel center and a proton to the coordinated silyl ligand, affording a species such as "[HSiP$^{iPr}_3$]Ni–H". Such a transformation would be analogous to the intramolecular heterolytic H_2 activation reported to be facile by Caulton and co-workers for the low-temperature intermediate [PNP]Ni$(H_2)^+$ (Scheme 3). However, no evidence for such a transformation is observed for **5a**. Indeed, even the addition of triethylamine fails to deprotonate the bound dihydrogen of **5a** to generate the neutral hydride species.

An alternative synthesis of the nickel hydride, [SiP$^{iPr}_3$]Ni–H (**6a**), is provided by reaction of the free ligand H[SiP$^{iPr}_3$] with Ni$(COD)_2$ (Scheme 4). We note in brief that hydride **6a** facilitates the isomerization of excess 1-octene at room temperature to generate both *cis*- and *trans*-2-octene. In contrast to **5a**, the coordinated dihydrogen of **5b** can be deprotonated by NEt_3 to generate the neutral hydride [SiP$^{Ph}_3$]Ni–H (**6b**), which can alternatively be synthesized directly from H[SiP$^{Ph}_3$] and Ni$(COD)_2$ (Scheme 4). Hydride **6b** also effects the isomerization of 1-octene to 2-octenes, though heating to 60 °C is required for an appreciable rate.

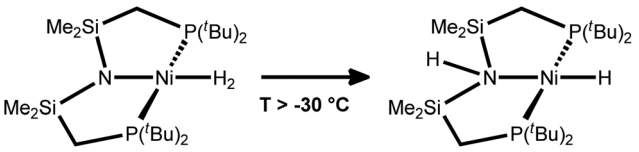

Scheme 3

The stability of these dihydrogen adducts presumably arises not only from the electrophilicity of the cationic metal center, but also from the steric and geometric requirements of the ligand, which orients the d_{z^2} LUMO into the axial coordination site, as well as from the electronic properties of the silyl anchor, which is neither basic enough to intramolecularly deprotonate the H_2 nor sufficiently Lewis acidic to accept a hydride. The fact that these nickel centers bind N_2 as well as H_2 is in contrast to the behavior of the electrophilic complex $[Mn(CO)_3(PCy_3)_2]^+$.[22] This cationic compound was shown to bind H_2 more strongly than its isoelectronic, neutral Cr analogue, due to increased σ-donation to the Mn center; it does not, however, appear to bind N_2 favorably.

These [SiP$^R_3$]Ni(H_2) adducts are structurally related to the previously reported {[SiP$^{iPr}_3$]Pt(H_2)}{BAr$^F_4$}, and also to a cationic iron(II) derivative, {[SiP$^{iPr}_3$]Fe(H_2)}{BAr$^F_4$}; the latter species is notably unusual due to its $S = 1$ ground state.[23] SiP$^R_3$ metal compounds thus seem to be particularly suited for stabilizing these types of H_2 adducts due to the electronic properties and geometric requirements of the ligand; the stabilities of these adducts are further modulated through a balance of ligand σ-bond donation and metal π back-bonding.

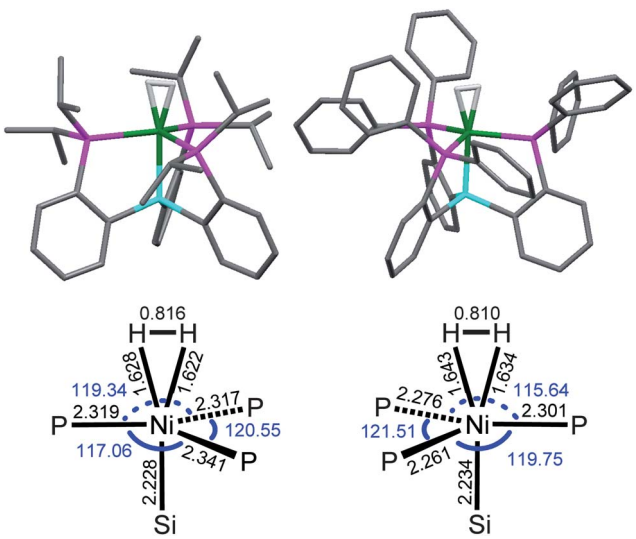

Fig. 5 DFT minimized structures and selected bond lengths (Å) and angles (°) of **5a** (left) and **5b** (right). Ligand hydrogen atoms omitted for clarity. See ESI† for computational details.

Comparison to an isoelectronic Ni boratrane system

A nickel tris(phosphino)boratrane complex, [TP^{iPr}B]Ni, has been reported by Bourissou and co-workers[24] and can be regarded as

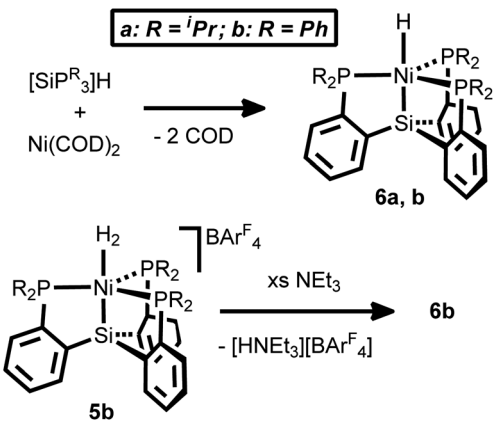

Scheme 4

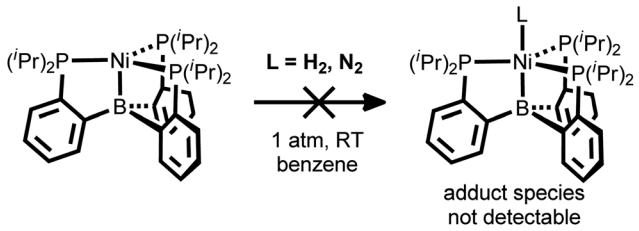

Scheme 5

valence isoelectronic to the $[SiP^{iPr}_3]Ni^+$ fragment. The reactivity of this compound with N_2 and H_2 had not been described; we were therefore interested in exploring this reactivity in order to contextualize the chemistry detailed herein. We wondered whether the neutral $[TP^{iPr}B]Ni$ species would be appreciably less electrophilic than $[SiP^{iPr}_3]Ni^+$, and hence not show a similarly strong affinity for H_2 and N_2, if σ-donation indeed dominates the binding interaction.

$[TP^{iPr}B]Ni$ was synthesized as reported, and its NMR spectra in benzene under an atmosphere of N_2 matched the published spectra (see ESI†). Additionally, no N–N stretch was observed in the solid state IR spectrum, and crystals grown under N_2 at −35 °C had the same unit cell as that previously reported for the four-coordinate $[TP^{iPr}B]Ni$. These data suggest that, unlike the isoelectronic $[SiP^{iPr}_3]Ni^+$ fragment, $[TP^{iPr}B]Ni$ does not bind N_2 at room temperature, at least not strongly enough to be detected (Scheme 5).

Only very slight shifts are seen in the RT ^1H and $^{31}P\{^1H\}$ NMR spectra when $[TP^{iPr}B]Ni$ is exposed to one atmosphere of H_2 (Fig. S8a, b, ESI†). However, the RT ^1H spectrum lacked the resonance corresponding to free H_2 in solution, which prompted further investigation of this reaction. We hypothesized that, in analogy to what is observed for **5b**, the lack of a free H_2 resonance in the $[TP^{iPr}B]Ni$ spectrum could be an indicator of a weak, fluxional interaction between the metal center and H_2. The VT ^1H and $^{31}P\{^1H\}$ NMR spectra of $[TP^{iPr}B]Ni$ under an H_2 atmosphere (Fig. S8c, d, ESI†) exhibit changes upon cooling that are distinct from those of the VT spectra reported for $[TP^{iPr}B]Ni$.[24] Though the $^{31}P\{^1H\}$ spectra indicate a conversion to a different species below −60 °C, free H_2 remains unobserved in the ^1H spectra. The identity of the low-temperature species has not yet been determined, but is likely the H_2-adduct.

DFT optimization of a hypothetical H_2 adduct of $[TP^{iPr}B]Ni$ supports this idea. The minimized structure of $[TP^{iPr}B]Ni(H_2)$ (**A**) (Fig. 6) features both a shorter H–H bond and longer Ni–H distances than the calculated $[SiP^R_3]Ni(H_2)$ adducts, which is consistent with much weaker binding of the dihydrogen. We conjecture that a more electron-poor Ni boratrane might result in a stronger interaction with N_2 and H_2; current efforts to experimentally test this hypothesis are in progress.

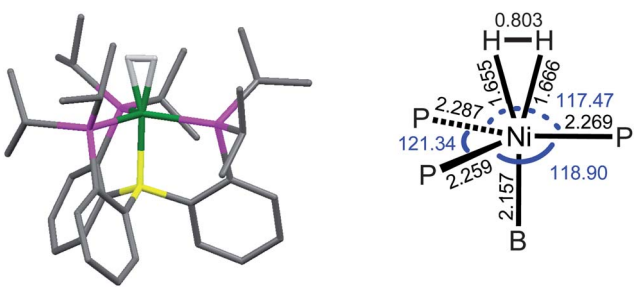

Fig. 6 DFT minimized structure and selected bond lengths (Å) and angles (°) of **A**. Ligand hydrogen atoms omitted for clarity. See ESI† for computational details.

Conclusions

We have demonstrated that cationic, Ni(II) complexes of tris(phosphino)silyl ligands $[SiP^R_3]^-$ are able to coordinate both dinitrogen and dihydrogen, generating among the first thermally stable examples of these types of compounds. We conjecture that stability of the N_2 compounds is predominantly due to the strength of the ligand σ-donation interaction, while π back-bonding from the metal appears to be relatively less significant. In the H_2 adducts, however, the effect of π back-bonding may be more pronounced. Further work is warranted to shed additional light on the interplay of sigma and pi effects in stabilizing complexes of these types. The dihydrogen adducts of nickel described above broaden the scope of stable dihydrogen compounds of late first-row transition metals, including Co, Ni, and Cu,[25,26] and are of interest with respect to hypotheses suggesting that Ni can serve as the site for H_2 binding and heterolytic activation in [NiFe] hydrogenases. Most notable is that H_2 has been demonstrated to bind to a highly electrophilic nickel center as a σ-adduct, and exhibits heterolysis upon addition of exogenous base.

Acknowledgements

This work was supported by the NSF (CHE-0750234) and the Gordon and Betty Moore Foundation. We are grateful to Dr Peter Müller and Dr Marc-Etienne Moret for assistance with XRD and DFT studies, respectively.

Notes and references

1 (*a*) G. J. Kubas, in *Metal Dihydrogen and σ-Bond Complexes: Structure, Theory, and Reactivity*, Kluwer Academic/Plenum Publishers, New York, 2001; (*b*) G. J. Kubas, *Chem. Rev.*, 2007, **107**, 4152; (*c*) D. M. Heinekey and W. J. Oldham, Jr., *Chem. Rev.*, 1993, **93**, 913.

2 (*a*) J. Niu, B. K. Rao and P. Jena, *Phys. Rev. Lett.*, 1992, **68**, 2277; (*b*) J. Niu, B. K. Rao, P. Jena and M. Manninen, *Phys. Rev. B: Condens. Matter*, 1995, **51**, 4475.

3 Selected examples: in bulk metal: (*a*) J.-Y. Carriat, C. Lepetit, M. Kermarec and M. Che, *J. Phys. Chem. B*, 1998, **102**, 3742; in gas phase: (*b*) P. R. Kemper, P. Weis and M. T. Bowers, *Chem. Phys. Lett.*, 1998, **293**, 503, and references therein; microporous materials: (*c*) M. Dinca and J. R. Long, *J. Am. Chem. Soc.*, 2007, **129**, 11172; under matrix-isolation: (*d*) R. L. Sweany, M. A. Polito and A. Moroz, *Organometallics*, 1989, **8**, 2305.

4 T. He, N. P. Tsvetkov, J. G. Andino, X. Gao, B. C. Fullmer and K. G. Caulton, *J. Am. Chem. Soc.*, 2010, **132**, 910.

5 (*a*) W. Lubitz, E. Reijerse and M. van Gastel, *Chem. Rev.*, 2007, **107**, 4331, and references therein; (*b*) J. C. Gordon and G. J. Kubas, *Organometallics*, 2010, **29**, 4682.

6 (*a*) M. Pavlov, P. E. M. Siegbahn, M. R. A. Blomberg and R. H. Crabtree, *J. Am. Chem. Soc.*, 1998, **120**, 548; (*b*) P. E. M. Siegbahn, J. W. Tye and M. B. Hall, *Chem. Rev.*, 2007, **107**, 4414.

7 See, for example: (*a*) M. Brecht, M. van Gastel, T. Buhrke, B. Friedrich and W. Lubitz, *J. Am. Chem. Soc.*, 2003, **125**, 13075; (*b*) H. Ogata, Y. Mizoguchi, N. Mizuno, K. Niki, S.-I. Adachi, N. Yasuoka, T. Yagi, O. Yamauchi, S. Hirota and Y. Higuchi, *J.*

Am. Chem. Soc., 2002, **124**, 11628; (*c*) M. Stein and W. J. Lubitz, *J. Inorg. Biochem.*, 2004, **98**, 862.
8 (*a*) D. Sellmann, F. Geipel and M. Moll, *Angew. Chem., Int. Ed.*, 2000, **39**, 561; (*b*) A. D. Wilson, R. K. Shoemaker, A. Miedaner, J. T. Muckerman, D. L. DuBois and M. R. DuBois, *Proc. Natl. Acad. Sci. U. S. A.*, 2007, **104**, 6951, and references therein; (*c*) S. Pfirrmann, S. Yao, B. Ziemer, R. Stösser, M. Driess and C. Limberg, *Organometallics*, 2009, **28**, 6855.
9 (*a*) H. Huber, E. P. Kündig, M. Moskovits and G. A. Ozin, *J. Am. Chem. Soc.*, 1973, **95**, 332; (*b*) C. A. Tolman, D. H. Gerlach, J. P. Jesson and R. A. Schunn, *J. Organomet. Chem.*, 1974, **65**, C23.
10 (*a*) P. W. Jolly, K. Jonas, C. Krüger and Y.-H. Tsay, *J. Organomet. Chem.*, 1971, **33**, 109; (*b*) R. Waterman and G. L. Hillhouse, *Can. J. Chem.*, 2005, **83**, 328; (*c*) S. Pfirrmann, C. Limberg, C. Herwig, R. Stösser and B. Ziemer, *Angew. Chem., Int. Ed.*, 2009, **48**, 3357.
11 D. Zhu, I. Thapa, I. Korobkov, S. Gambarotta and P. H. M. Budzelaar, *Inorg. Chem.*, 2011, **50**, 9879.
12 (*a*) C. W. DeKock and D. A. VanLeirsburg, *J. Am. Chem. Soc.*, 1972, **94**, 3235; (*b*) G. A. Ozin and W. E. Klotzbücher, *J. Am. Chem. Soc.*, 1975, **97**, 3965; (*c*) B. V. Lokshin and I. I. Greenwald, *J. Mol. Struct.*, 1990, **222**, 11; (*d*) A. J. Bridgeman, O. M. Wilkin and N. A. Young, *Inorg. Chem. Commun.*, 2000, **3**, 681.
13 N. P. Mankad, M. T. Whited and J. C. Peters, *Angew. Chem., Int. Ed.*, 2007, **46**, 5768.
14 C. Tsay, N. P. Mankad and J. C. Peters, *J. Am. Chem. Soc.*, 2010, **132**, 13975.
15 M. T. Whited, N. P. Mankad, Y. Lee, P. F. Oblad and J. C. Peters, *Inorg. Chem.*, 2009, **48**, 2507.
16 T. Yamabe, K. Hori, T. Minato and K. Fukui, *Inorg. Chem.*, 1980, **19**, 2154.
17 This effect is also observed, for example, in tris(perfluoroalkyl) borane carbonyls which exhibit C–O stretching frequencies higher than that of free CO in addition to solid-state C–O distances shorter than in free CO. See: (*a*) A. J. Lupinetti, S. H. Strauss and G. Frenking, *Prog. Inorg. Chem.*, 2001, **49**, 1; (*b*) M. Gerken, G. Pawelke, E. Bernhardt and H. Willner, *Chem.–Eur. J.*, 2010, **16**, 7527.
18 Libration of the terminal N_2 moiety may also contribute to the short N–N distances obtained from the crystal structures of **2a** and **2b**, which are shorter than the 1.0975 Å observed for free N_2. See: P. Müller in *Crystal Structure Refinement*, ed. P. Müller, Oxford University Press, Oxford, 2006, pp. 151–152.
19 For some examples of Ni(II) carbonyl complexes, see: (*a*) J. J. Bishop and A. Davison, *Inorg. Chem.*, 1971, **10**, 832; (*b*) M. Wada and K. Oguro, *Inorg. Chem.*, 1976, **15**, 2346; (*c*) A. Miedaner, C. J. Curtis, S. A. Wander, P. A. Goodson and D. L. DuBois, *Organometallics*, 1996, **15**, 5185.
20 A. L. DeLacey, C. Stadler, V. M. Fernandez, E. C. Hatchikian, H.-J. Fan, S. Li and M. B. Hall, *JBIC, J. Biol. Inorg. Chem.*, 2002, **7**, 318.
21 R. H. Crabtree, *Acc. Chem. Res.*, 1990, **23**, 95.
22 A. Toupadakis, G. J. Kubas, W. A. King, B. L. Scott and J. Huhmann-Vincent, *Organometallics*, 1998, **17**, 5315.
23 Y. Lee, R. A. Kinney, B. M. Hoffman and J. C. Peters, *J. Am. Chem. Soc.*, 2011, **133**, 16366.
24 M. Sircoglou, S. Bontemps, G. Bouhadir, N. Saffron, K. Miqueu, W. Gu, M. Mercy, C.-H. Chen, B. M. Foxman, L. Maron, O. V. Ozerov and D. Bourissou, *J. Am. Chem. Soc.*, 2008, **130**, 16729.
25 T. J. Hebden, A. J. St. John, D. G. Gusev, W. Kaminsky, K. I. Goldberg and D. M. Heinekey, *Angew. Chem., Int. Ed.*, 2011, **50**, 1873.
26 Dihydrogen complexes of copper have been detected in Cu-doped ZnO and in Ar matrices: (*a*) E. V. Lavrov, J. Weber and F. Börrnert, *Phys. Rev. B: Condens. Matter Mater. Phys.*, 2008, **77**, 155209; (*b*) S. Plitt, M. R. Bär, R. Ahlrichs and H. Schnöckel, *Angew. Chem., Int. Ed. Engl.*, 1991, **30**, 832.

